Low-Temperature Specific Heats of Titanium, Zirconium, and Hafnium

G. D. Kneip, Jr.,* J. O. Betterton, Jr., and J. O. Scarbrough

Metals and Ceramics Division, Oak Ridge National Laboratory,† Oak Ridge, Tennessee

(Received 2 November 1962)

The specific heats of titanium, zirconium, and hafnium were found to obey the relation $c = \gamma T + \beta T^3$ from 1.1 to 4.5°K within the experimental error. As in other transition metals, the electronic term is large and for the Group IV-A metals decreases with increasing atomic number indicating a progressively larger degree of electronic interaction in the sequence titanium, zirconium, and hafnium. The Debye temperatures decrease with increasing atomic mass as would be expected from the central-force model; however, the ratio of the Debye temperatures indicate that the average atomic force constant for hafnium is some 50% larger than for titanium and zirconium in agreement with the unusually small atomic volume of hafnium.

INTRODUCTION

THE results of previous measurements[1,2] of the low-temperature specific heats of the Group IV-A metals titanium, zirconium, and hafnium show a large scatter for the coefficient of the electronic term and for the Debye temperatures. Recently, the temperature scale in the liquid-helium range has been better established[3,4] and the experimental techniques and apparatus have been improved to such an extent that specific heats can be measured in the liquid-helium temperature range with an expected uncertainty of less than ±1%.[5] In addition, these metals are now available with a higher purity in sufficient amounts for the low-temperature measurements. Titanium, zirconium, and hafnium, whose electronic structure in the free atom consists of two s and two d electrons outside an inert gas configuration, occur early in the three long periods of transition elements. The electronic structures of these metals consist of overlapping, partially filled, s and d bands arising from the closely spaced atomic s and d states. In the one-electron approximation the electronic specific heats are proportional to the sum of the density of states of the s and d bands at the Fermi surface. Because d bands are narrow and have a relatively high density of states compared to s and p bands, the electronic specific heats of these elements are higher than those of the non-transition elements which have the same number of electrons outside of closed shells. The electronic specific heats of these three metals are approximately equal since the factors which determine the band structure are similar. Thus, for all three, the field produced by the nucleus and the closed shell electrons is approximately the same, the equilibrium lattice structure is hexagonal close packed with an axial ratio of approximately 1.59 and the atomic volumes are regular except for hafnium which has a newly completed $4f$ shell. Although the Born-von Kármán theory of lattice dynamics has been applied to a central force model of a hexagonal metal,[6,7] the Debye temperatures of the Group IV-A metals cannot be computed on this basis for comparison with the specific heats because the elastic constants of these metals at low temperatures are unknown. A less accurate comparison between the elastic properties and the specific heats may be made by assuming that the Debye approximation is valid below 4°K and that the metals are isotropic.[8] The Debye temperatures can then be related to Young's modulus and Poisson's ratio which are reasonably well known for these metals. The Debye temperatures computed in this manner are in substantial agreement with the measured specific heats.

EXPERIMENTAL DETAILS

The specific heats were measured at approximately 35 points from 1.2 to 4.5°K in the customary manner by thermally isolating the specimen from the helium bath, applying a known electrical energy input and observing the temperature rise of the sample. The specific heat at the mean temperature of the heating pulse, then, is computed from the equation

$$c = \frac{1}{m}\left(\frac{eit}{\Delta T} - C_a\right), \tag{1}$$

where m is the specimen mass, ΔT the temperature rise, eit the energy input, and C_a the heat capacity of the thermometer and heater at the mean temperature of the heating pulse. A mechanical switch consisting of a copper rod tipped with indium which could be pressed against the sample was used to establish thermal contact between the specimen and the bath to cool the specimen to 1.2°K as shown in Fig. 1. The thermometer, a 56-Ω, 1/10-W Allen Bradley carbon resistor, and the heater, approximately 1200 Ω of 1.5-mil Manganin wire, were

* Present address: SUPERCON, Houston, Texas.
† Operated by the Union Carbide Corporation for the U. S. Atomic Energy Commission.
[1] N. M. Wolcott, in *Conference de physique des basses temperature, Paris, 1955* (Centre National de la Recherche Scientifique, and UNESCO, Paris, 1956), p. 286.
[2] I. Estermann, S. H. Friedberg, and J. E. Goldman, Phys. Rev. 87, 582 (1952).
[3] J. R. Clement, J. K. Logan, and J. Gaffney, Phys. Rev. 100, 743 (1955).
[4] H. Van Dijk and M. Durieux, Physica 24, 920 (1958).
[5] W. S. Corak, M. D. Garfunkel, C. B. Satterthwaite, and A. Wexler, Phys. Rev. 98, 1699 (1955).

[6] L. J. Slutsky and C. W. Garland, J. Chem. Phys. 26, 787 (1957).
[7] C. W. Garland and L. J. Slutsky, J. Chem. Phys. 28, 331 (1958).
[8] J. C. Slater, *Introduction to Chemical Physics* (McGraw-Hill Book Company, Inc., New York, 1939), p. 234.
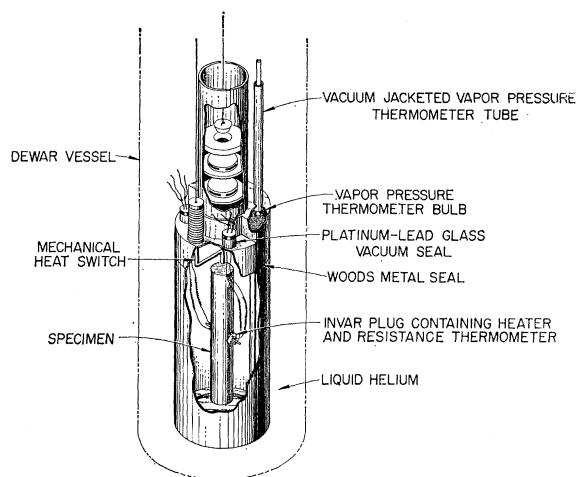
FIG. 1. Low-temperature part of the cryostat.

cemented into a tapered Invar plug which was pressed into a matching hole in the specimen. The temperature rise of the sample and the mean temperature were obtained by extrapolating the resistance vs time curves to the center of the heating period to obtain the initial and final resistance, computing the initial and final temperature from a two-constant form of the Clement empirical relation,[9] and applying a correction from a deviation curve obtained from the thermometer calibration.

At the conclusion of the specific heat measurements on each sample, the thermometer resistance was calibrated against the vapor pressure of liquid helium using the vapor pressure-temperature scale of Van Dijk and Durieux. Approximately 10 μ of helium gas was added to the specimen chamber at this time (but not earlier to avoid spurious helium effects) in order to provide thermal coupling between the specimen, the vapor pressure thermometer bulb, and the helium bath. Above the lambda point of liquid helium, the vapor pressure thermometer was used so that hydrostatic head corrections were unnecessary while below the lambda point the pressure at the top of the Dewar was measured. To facilitate the computation of the temperature, a resistance temperature was defined by

$$T_R = \ln R / (0.68748 \ln R - 1.09288)^2, \qquad (2)$$

where the constants were chosen so that the resistance temperature approximately coincided with[4] T_{58} from 2 to 4°K and the thermometer calibration data were used to construct a deviation curve $T_{58} - T_R$ vs T_R for each experiment. Several deviation curves where each point represents the average of at least two measurements are shown in Fig. 2 to illustrate the reproducibility of the thermometer. The small shifts in the deviation curve for different experiments are apparently caused by strains introduced in the thermometer by the necessary handling in changing from one specimen to another or by thermal contraction when the sample is cooled from room temperature, as repeated calibrations in the same specimen do not show this effect if the specimen is not warmed above 4.2°K.

The heat capacity of the Invar plug containing the heater and thermometer was determined as a function of temperature by measuring the heat capacity of the plug plus that of three different copper specimens (0.03006, 0.60904, and 1.4643 moles). The specific heat of copper was assumed to be of the usual form

$$c = \gamma T + \beta T^3, \qquad (3)$$

and that of the addendum to be

$$c_a = \gamma_a T + \beta_a T^3. \qquad (4)$$

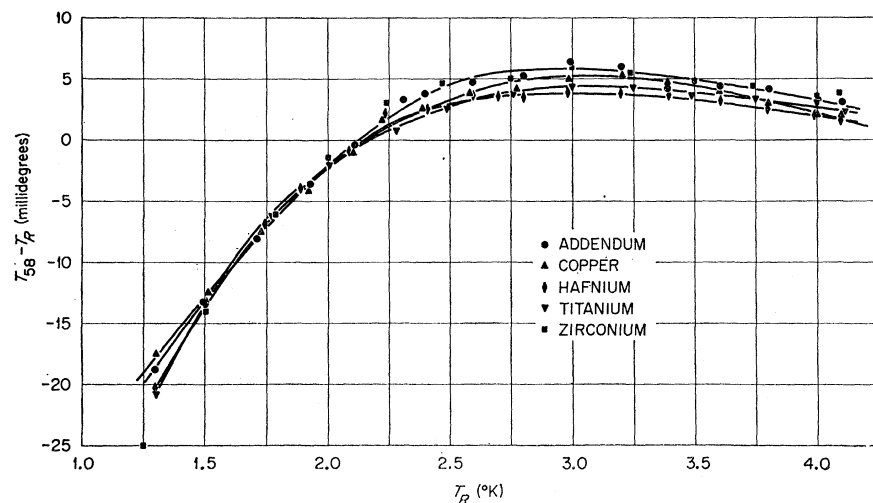The four constants, γ and β for copper and γ_a and β_a for

FIG. 2. Thermometer deviation curves.

[9] J. R. Clement and E. H. Quinnell, Rev. Sci. Instr. 23, 213 (1952).

TABLE I. Sources and heat treatments of calorimeter specimens.

| Specimen | | Copper | | Titanium | | Zirconium | | | Hafnium |
	Cu-1	Cu-2	Cu-3	Ti	Zr-1	Zr-2	Zr-3	Zr-4	Hf
Source	a	a	a	b	c	a	d	c	e
Melting	Vacuum	∼10⁻⁶ mm Hg crucible	Graphite	No	No	Argon	Arc	No	Argon arc
Hydrogen removal treatment	...	...	...	1100°C until pressure reached 1×10⁻⁶ mm Hg					
Homogenization anneal									
Temperature (°C)	1000	1000	1000	None	None	1100	None	None	None
Time	1 h	1 h	1 h			7 days			
Final anneal									
Temperature (°C)	800	800	800	800	800	845	800	1100	800
Time	1 h	1 h	1 h	1 h	1 h	25 days	2 h	1 h	1 h
Cooling rate	Slow	Slow	Slow	Slow	Slow	Slow	Slow	Water quench	Slow
Specimen size	1.4643	0.60904	0.03006	0.88359	0.72051	0.79390	0.90033	0.58476	0.40035

a American Smelting and Refining Company High Purity 99.999% Cu.
b New Jersey Zinc Company.
c Westinghouse Atomic Power Division, Lot 1.
d Westinghouse Atomic Power Division, Lot 2.
e Battelle Memorial Institute.

the addendum, were then found by a least-squares fit of the data from the three experiments to the equation

$$c = m(\gamma T + \beta T^3) + \gamma_a T + \beta_a T^3. \qquad (5)$$

The heat capacity of the addendum deviates very slightly from the assumed $T + T^3$ temperature dependence at the lowest temperatures and smoothed experimental values of the addendum heat capacity were used in the computation of the specific heats of the metal specimens. The heat capacity of the addendum amounts to 5.3% of the heat capacity of a 1-mole metal specimen at 1.3°K and 4.5% at 4.2°K.

In addition to the uncertainties in the measured quantities of Eq. (1), the error caused by the non-linearity of the specific heat as a function of temperature and the error in the value of the mean temperature which is assigned to the value of the specific heat computed from Eq. (1) must be considered. The error due to the nonlinearity of the specific heat is made less than 0.01% by using ΔT's of 50 mdeg and less. The error in the mean temperature may be taken as equal to the error in temperature in a single measurement of the temperature and is approximately ±2 mdeg. This value is in agreement with the scatter shown in the thermometer calibration curves of Fig. 2. The errors in the terms of Eq. (1) may all be made small in relation to the error in ΔT so that the uncertainty in the specific heat is determined by ΔT. Thus, the random error of an individual specific-heat measurement is determined by the precision with which ΔR can be measured, in this case approximately 0.1%. Systematic errors can arise in the calibration of the resistance thermometer from the method used to measure the vapor pressure of the liquid helium, and are estimated to be of the order 0.1%.

Metal Specimens

Specimens approximately $\frac{3}{4}$ in. diam and 1–3 in. long suitable for the calorimeter were prepared from high-purity copper and from iodide process titanium, zirconium, and hafnium. The source of the materials as well as their heat treatments are listed in Table I. The copper specimens were annealed in a graphite boat in a continuously pumped vacuum furnace at pressures of approximately 10⁻⁶ mm of Hg. All of the annealing of the titanium, zirconium, and hafnium specimens, except the long-time anneals of Zr-2, was carried out in a high-frequency induction furnace at pressures of approximately 1×10⁻⁶ mm of Hg with the specimen suspended by a tungsten wire to prevent reaction of the hot specimen with the vacuum walls. Contamination of specimen Zr-2 during heat treatment was prevented by wrapping the specimen in zirconium foil and then sealing it in an evacuated quartz capsule. The resulting specimens are of at least 99.9% purity and the significant impurity concentrations are listed in Table II. The values listed

TABLE II. Impurity content of specific heat specimens.

Impurity	Titanium	Zr-1 Zr-4	Zr-2	Zr-3	Hafnium
		Specimen			
Ti	99.86%	NAᵃ	NA	NA	NA
Zr	180–700 ppm	99.95%	99.95%	99.95%	500 ppm
Hf	NA	130 ppm	NA	NA	99.95%
Mg	<100 ppm	NA	NA	NA	NA
Si	3	2 ppm	14	15	65ppm
Cr	NA	2	NA	7	NA
Fe	200	23	55	70	200
Ni	<4	11	NA	14	7
Cu	2.4	0.8	13	3	3
Mo	4	4	NA	25	43
W	2	0.4	8	8	1
H₂	<1 ppm	<1 ppm	11	<1	<1
N₂	9	3	<5	<5	<5
O₂	100	26	74	10	18
C	190	56	30	80	130
Vickers hardness	63	63	68	75	120

a Not analyzed.

TABLE III. Low-temperature specific heats of copper.

Specimen	Specimen purity (%)	γ (mJ/mole deg²)	θ_D (°K)	Temperature scale	Reference
Cu-1	99.999	0.697±0.007	345.1±1.4	T_{58}[a]	
Cu-2	99.999	0.696±0.007	342.3±1.4	T_{58}	
Cu	99.999	0.688±0.002	343.8±0.5	T_{55E}[b]	f
Cu	99.999	0.686±0.005	345.1±0.9	T_{49C}[c]	g
Cu	99.999	0.69	342	T_{55E}, T_{55L}[d]	h
Cu	99.99	0.691	347 ±2	T_{55E}	i
Cu	99.6	0.75	315	T_{37}[e]	j
Cu	99.9	0.74	335		k

a See reference 4.
b See reference 3.
c H. Van Dijk and D. Shoenberg, Nature 164, 151 (1949) as corrected by R. A. Erickson and L. D. Roberts, Phys. Rev. 93, 957 (1954).
d H. Van Dijk and M. Durieux, in *Conference de physique des basses température, Paris, 1955* (Centre National de Recherche Scientifique, and UNESCO, Paris, 1956), p. 595.
e G. Schmidt and W. H. Keesom, Physica 4, 963 (1937)
f See reference 5.
g J. A. Rayne, Australian J. Phys. 9, 189 (1956).
h N. E. Phillips, in *Proceedings of the Fifth International Conference on Low Temperature Physics and Chemistry* (University of Wisconsin Press, Madison, Wisconsin, 1958), p. 414.
i M. Griffel, R. W. Vest, and J. F. Smith, J. Chem. Phys. 27, 1267 (1957).
j See reference 2.
k W. H. Keesom and J. A. Kok, Physica 3, 1035 (1936).

for the metallic impurities were obtained by neutron-activation analyses, the interstitial gases by vacuum fusion, and carbon by the combustion method. Filings from the titanium and hafnium specimens and one of the zirconium specimens were found to be hexagonal close packed at 4.2°K upon examination with an x-ray diffractometer,[10] indicating that there are no phase changes in these metals between 4.2 and 300°K.

RESULTS

The specific heat of copper from 1.2 to 4.5°K was measured in the same experiments that determined the heat capacity of the thermometer and heater assembly. The specific heat of copper has also been measured carefully at a number of other laboratories allowing a comparison to be made between the results of experiments carried out independently in different cryostats and evaluation of the differences to be expected in the

coefficient of the electronic term of the specific heat and in the Debye temperature. Table III lists these values for copper with the probable errors, where the authors have given them, as well as the results of the present experiments. The electronic coefficient and the Debye temperatures were determined by a least-square fit of the data to the equation

$$c = \gamma T + \beta T^3, \qquad (6)$$

where $\theta = (12\pi^4 R/5\beta)^{1/3}$. The limits of error shown for the electronic coefficient are the confidence limits at the 99% confidence level to which one-half of 1% of gamma has been arbitrarily added to allow for systematic errors. Because of the manner in which the curve fitting was done, the error limits shown for the Debye temperatures are not true confidence limits. These limits were derived from the confidence limits on beta and include an allowance of one-half of 1% to allow for systematic

TABLE IV. Low-temperature specific heats of the group IV-A metals.

Specimen	Specimen purity (%)	γ (millijoules/mole deg²)	θ_D (°K)	Temperature scale	Reference
Ti	99.86	3.346±0.026	427 ±5	T_{58}	
		3.351±0.029	430 ±6		
Ti	99.98	3.56	430		1
Ti	99	3.35	280	T_{37}	2
Zr-1	99.95	2.798±0.023	290.9±1.3	T_{58}	
		2.792±0.023	291.2±1.3		
Zr-2	99.95	2.827±0.028	292.6±1.3	T_{58}	
Zr-3	99.95	2.804±0.026	291.3±1.3	T_{58}	
Zr-4	99.95	2.813±0.022	292.8±1.2		
		2.808±0.024	291.2±1.3	T_{58}	
Zr	2% Hf	3.03	310		1
Zr	99.5	2.90	265	T_{37}	2
Hf	99.95	2.159±0.022	252.3±0.9		
		2.167±0.028	251.5±1.2	T_{58}	
Hf	99.98	2.64	261		1

10 We are indebted to J. C. Ogle of the Metals and Ceramics Division for carrying out the low-temperature x-ray examination.

errors. Both the electronic coefficients and Debye temperatures for copper agree within the limits of error for the measurements reported since 1955 showing the very close agreement that can be obtained on materials of high purity. The specific heat of copper deviates from Eq. (6) by less than 0.2% except possibly at the lowest temperatures where the thermometer calibration is least certain. The deviation at the lower temperatures is of the opposite sense but about the same magnitude of that observed by Phillips for aluminum using essentially the same temperature scale. This deviation of copper and aluminum[11] from Eq. (6) probably should be attributed to the experimental difficulty in thermometer calibration rather than failure of the T, T_3 model or inaccuracies in the helium vapor pressure-temperature scale.

Table IV lists the electronic coefficient of the specific heat and the Debye temperatures for the Group IV-A metals. Titanium, zirconium, and hafnium were found to obey the T,T^3 relationship within the experimental error as shown in Fig. 3, where c/T is plotted as a function of T^2. Some of the physical properties of these elements are sensitive to trace amounts of impurities; for instance, the allotropic transformation of this zirconium takes place over a 10 to 15°C temperature interval and for this reason the specific heat of several zirconium samples has been measured to establish the effect of small variations in the impurity content. The Zr-1 specimen is iodide crystal bar which has been annealed in an evacuated quartz capsule below the allotropic transformation temperature and then slowly cooled to room temperature. The Zr-2 sample was prepared in a similar manner except that it was arc melted first to serve as a control for alloying experiments. The Zr-3 specimen was prepared from a second batch of zirconium in a similar manner to the Zr-1 specimens. The Zr-4 was water quenched from above the allotropic transformation temperature to induce lattice distortions. In zirconium, of course, the high-temperature bcc phase is not retained even with very rapid cooling rates but transforms to a distorted hcp structure which has the same lattice parameters as the equilibrium alpha phase.

There is no significant difference in either the electronic specific heats or the Debye temperatures for the different zirconium samples, indicating that small variations in the amounts of impurities do not affect these measurements and that from the standpoint of the electronic and vibrational specific heats the metastable α' and the equilibrium α structures are equivalent. Thus, in contrast to the thermodynamic properties, the Debye temperatures and electronic specific heats of the Group IV-A elements are insensitive to changes in the impurity concentration in the ppm range and the present data from metals of 99.9% purity are believed to correctly represent the properties of the pure elements.
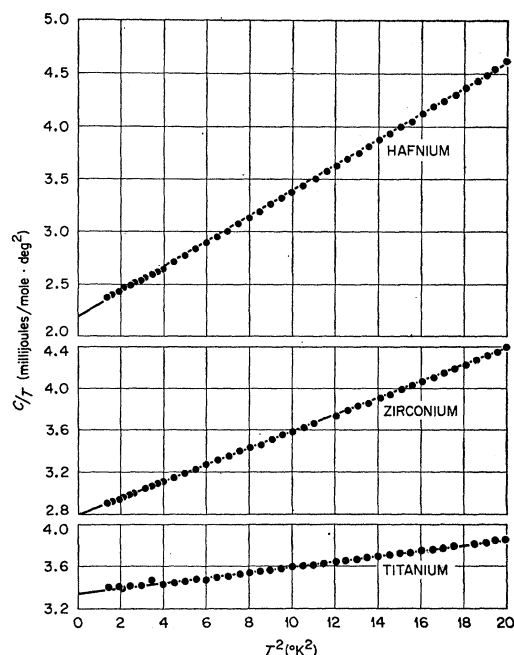
[11] N. E. Phillips, Phys. Rev. 114, 676 (1959).

FIG. 3. The specific heats of titanium, zirconium, and hafnium.

Both the electronic specific heats and the Debye temperatures decrease with increasing atomic number through the sequence titanium, zirconium, and hafnium. Figure 4 shows this variation in a schematic way. The Debye temperatures have been adjusted for the atomic
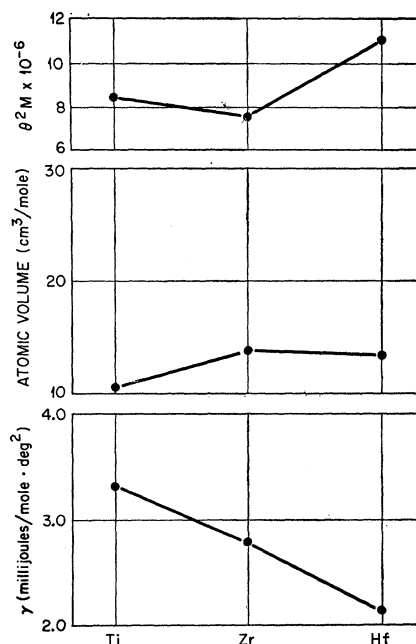

FIG. 4. Electronic specific heat, reduced Debye temperatures, and atomic volumes of the Group IV-A metals.

mass by plotting the product $M\theta^2$ so that they correspond to an average interatomic force constant in a central-force model of lattice vibrations. It is apparent that the force constant for hafnium is considerably larger than the force constants for the other three metals. The atomic volume of hafnium also is unusually small as shown in the second curve in the figure as a result of the lanthanide contraction which accompanies the filling of the $4f$ shell. This contraction is due to a stronger field acting upon the valence electrons as a result of the incomplete screening by the $4f$ electrons of the increased nuclear charge and results in increased binding forces. Thus the high force constant for hafnium is believed to be principally due to the lanthanide contraction. Electrons in both s and d bands contribute to the electronic specific heat. Since the s-wave functions are more

penetrating, the bottom of the s band should be lowered with respect to the bottom of the d band by increasing nuclear charge. In terms of the two-band model then, this would result in a smaller number of electrons in the d band, and hence, a decreasing electronic specific heat with increasing nuclear charge. Strictly speaking, this is only true if a decrease in the density of states in the d band occurs with a decrease in the number of electrons in the band but experimental evidence from zirconium alloys indicates this to be a reasonable assumption. As a result of the lanthanide contraction, the s and d wave functions should overlap to a great extent in hafnium and, therefore, the density of states should be reduced still further. The figure shows that this effect must be small, however, compared to the shift in position of the s and d bands.

Electrically Induced Nuclear Resonance in Al₂O₃ (Ruby)

Toshimoto Kushida and A. H. Silver

Scientific Laboratory, Ford Motor Company, Dearborn, Michigan

(Received 28 January 1963)

The application of an electric field to a crystalline lattice will, in general, produce an optical mode distortion. This lattice distortion will contribute to the electric field gradient tensor at the positions of the various atoms in the lattice. By applying an oscillating electric field to a single crystal of α-Al$_2$O$_3$ we have induced $\Delta m = \pm 2$ transitions for the Al^{27} nuclear spins. These "quadrupole" transitions were observed with a nuclear double resonance technique at 4.2°K. An rf electric field orthogonal to the trigonal axis of the crystal induced an oscillating asymmetry parameter η in the electric field gradient tensor. The magnitude of η as determined from the transition probability is $1.5\times10^{-7}/$(V/cm). The transient behavior as well as the steady-state populations were observed following the application and removal of the rf electric field. The initial slope of the signal following the application of the electric field was used to determine the quadrupole transition probability, and the remaining transient response was interpreted qualitatively in terms of the normal modes of the relaxation. These modes were derived from the rate equations which included the external driving terms. The line shape for the $\Delta m = \pm 2$ nuclear electric resonance was observed indirectly and is more than twice as broad as the dipolar lines with a distinct asymmetry. The width and shape are interpreted in terms of the nuclear dipole-dipole interaction.

I. INTRODUCTION

THE application of an electric field to a crystalline lattice will produce an optical mode distortion of the lattice. This electric polarization of the lattice will produce an associated internal electric field and its corresponding spacial derivatives. Bloembergen[1] has pointed out that for nuclei or paramagnetic ions in a lattice whose sites lack inversion symmetry, an externally applied electric field E produces a change in the quadrupole coupling constants or in the crystalline field splittings which are proportional to E. Such changes in the nuclear quadrupole coupling were first observed as a frequency shift or a broadening of the nuclear quadrupole resonance line.[2,3] This linear electric

field shift has also been observed in paramagnetic resonance spectra.[4,5]

Bloembergen[1] also suggested that if an oscillating electric field whose frequency matches the resonance condition is applied, transitions may be induced at a rate proportional to E^2. This effect has been observed by means of a change in the nuclear free induction decay signal for Ga^{69}, Ga^{71}, and As^{75} in GaAs when electric quadrupole transitions, $\Delta m = \pm 2$, were induced by means of an external electric field.[6]

[1] N. Bloembergen, Science **133**, 1363 (1961).

[2] T. Kushida and K. Saiki, Phys. Rev. Letters **7**, 9 (1961).

[3] J. Armstrong, N. Bloembergen, and D. Gill, Phys. Rev. Letters **7**, 11 (1961).

[4] G. W. Ludwig and H. H. Woodbury, Phys. Rev. Letters **7**, 240 (1961); J. O. Artman and J. C. Murphy, Bull. Am. Phys. Soc. **7**, 14 (1962).

[5] E. B. Royce and N. Bloembergen, Bull. Am. Phys. Soc. **7**, 200 (1962). After completion of this experiment, Bloembergen has kindly informed us that R. Dixon has observed the dc electric field effect on Al^{27} NMR lines in Al$_2$O$_3$. This was accomplished by using as much as 300 kV/cm. We would like to acknowledge the valuable comment given by Professor N. Bloembergen.

[6] E. Brun, R. Hann, W. Pierce, and W. H. Tanttila, Phys. Rev. Letters **8**, 365 (1962).